Stress States in Tramway Rails Predicted through a Principle of Virtual Power-Based Beam Theory Approach

Patricia Hasslinger, Aleš Kurfürst, Stefan Scheiner*, Christian Hellmich

Institute for Mechanics of Materials & Structures
TU Wien — Vienna University of Technology
Karlsplatz 13/202, 1040 Vienna, Austria

* Presenting author. Contact via ✉ stefan.scheiner@tuwien.ac.at / ☎ +43 1 58801 20265

Motivation and Outline

Tramways are an important means of transport in many urban areas, and mechanical failures of tramway rails, which may have been in operation for a substantial amount of time (a service life of several decades is not uncommon) can adversely affect daily life. However, studies elucidating the potentially crack- and failure-inducing stress states in tramway rails are surprisingly rare. On the one hand, realistic, full 3D Finite Element analyses of (tramway) rails are still expensive, both in terms of preparatory work and required computational power. On the other hand, classical beam theory approaches (Euler-Bernoulli bending, Saint-Venant torsion) may not be able to realistically represent the quite complex structural mechanical behavior of tramway rails. Namely, typical cross sections, as the one depicted in Figure 1, appear as being very compliant when subjected to torsional loading; and corresponding warping deformations are believed to induce stress states which are not considered in classical beam theories.

The overall objective of the presented work was developing a computationally efficient and theoretically sound modeling tool allowing for computing stress states tramway rails must withstand when subjected to operation-representing loading conditions. For that purpose, we chose a non-standard approach going beyond the state of the art in beam mechanics [1], involving rigorous utilization of the principle of virtual power [2,3], as briefly described below.

Figure 1: Photograph of a rail typically used in the Viennese tramway network, being of profile Ri60R1.

Theoretical Foundation based on Reformulating Beam Theory

Fundamentals of the principle of virtual power:

The principle of virtual power (PVP) expresses the balance between the virtual powers performed by external and internal forces. For a continuum, it reads as [2]

$$\underbrace{\int_V \mathbf{f}(\mathbf{x})\cdot\hat{\mathbf{v}}(\mathbf{x})\,\mathrm{d}V + \int_S \mathbf{T}(\mathbf{x})\cdot\hat{\mathbf{v}}(\mathbf{x})\,\mathrm{d}S}_{\mathcal{P}^{\text{ext}}} - \underbrace{\int_V \boldsymbol{\sigma}(\mathbf{x}):\hat{\mathbf{d}}(\mathbf{x})\,\mathrm{d}V}_{\mathcal{P}^{\text{int}}} = 0$$

with $\mathcal{P}^{\text{ext}}$ and $\mathcal{P}^{\text{int}}$ as the virtual powers performed by external and internal forces, V and S as the volume and surface of the considered domain, $\mathbf{x}$ as position vector, $\mathbf{f}$ as volume force vector, $\hat{\mathbf{v}}$ as virtual velocity field, $\mathbf{T}$ as traction force vector, $\boldsymbol{\sigma}$ as stress tensor, and $\hat{\mathbf{d}}$ as virtual Eulerian strain rate tensor.

Virtual beam kinematics:

A beam is considered fulfilling the classical Bernoulli assumptions [4], and the well-known Euler-Bernoulli kinematics are extended by torsional deformation, in line with [1], yielding the following virtual velocity components (in a Cartesian base system):

$$\begin{aligned}
\hat{v}_x(x,y,z) &= \hat{v}_x^{\text{GC}}(x) - \frac{\mathrm{d}\hat{v}_y^{\text{GC}}(x)}{\mathrm{d}x}y - \frac{\mathrm{d}\hat{v}_z^{\text{GC}}(x)}{\mathrm{d}x}z + \frac{\mathrm{d}\hat{\omega}_x(x)}{\mathrm{d}x}\psi_{\text{I}}(y,z) + \frac{\mathrm{d}^3\hat{\omega}_x(x)}{\mathrm{d}x^3}\psi_{\text{II}}(y,z)\\
\hat{v}_y(x,y,z) &= \hat{v}_y^{\text{GC}}(x) - \hat{\omega}_x(x)\left[z - z_{\text{CT}}\right]\\
\hat{v}_z(x,y,z) &= \hat{v}_z^{\text{GC}}(x) + \hat{\omega}_x(x)\left[y - y_{\text{CT}}\right]
\end{aligned}$$

with $\hat{v}_x$, $\hat{v}_y$, $\hat{v}_z$ as virtual velocities, $\hat{v}_x^{\text{GC}}$, $\hat{v}_y^{\text{GC}}$, $\hat{v}_z^{\text{GC}}$ as virtual velocities of the geometrical center, x, y, z as coordinates relating to the geometrical center, y_{CT}, z_{CT} as coordinates of the center of twist, ψ_{I}, ψ_{II} as primary warping function (representing St. Venant torsion) and secondary warping function (considering the effect of restrained warping), and $\hat{\omega}_x$ as virtual angular velocity.

The virtual Eulerian strain rate tensor follows straightforwardly from the virtual velocity field, through the well-known linearized relations.

Consideration of elastic support:

As further novelty, the (continuous) elastic support a tramway rail is resting on is considered through considering a further traction force acting onto the bottom contact face of the rail:

$$T_z^{\text{ES}}(x,y) = -k\left[u_z^{\text{GC}}(x) + \omega_x(x)\,(y - y_{\text{CT}})\right]$$

with u_z^{GC} being the displacement of the geometric center perpendicular to the contact face, and k the foundation modulus.

Force quantities, equilibrium and boundary conditions:

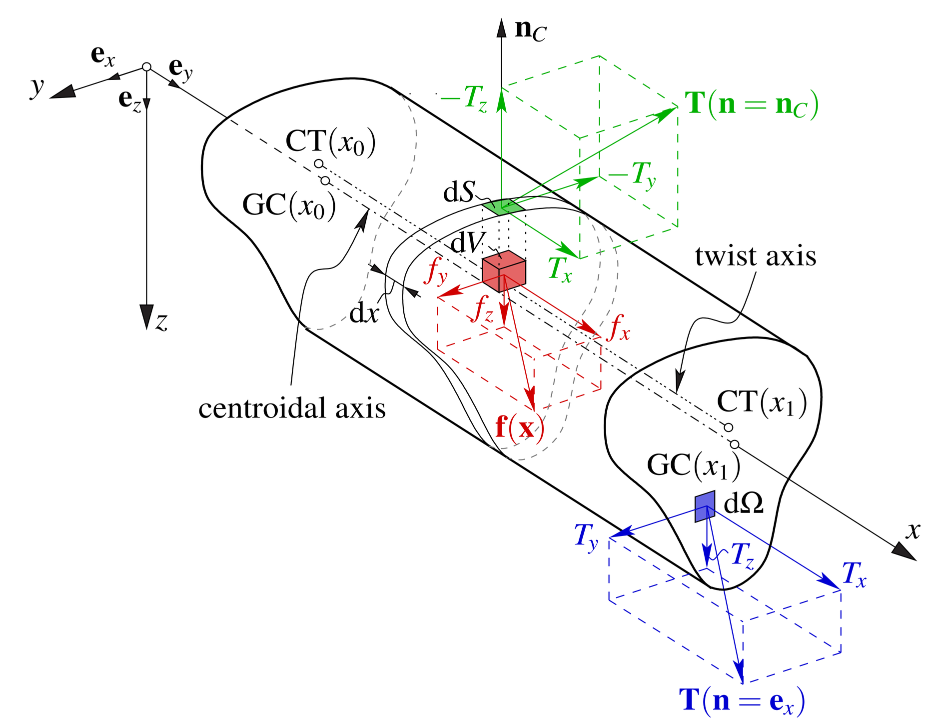

Figure 2: Considered beam, including base system, geometric center GC and center of twist CT, as well as traction force vectors and volume force vector.

Insertion of (i) linearized beam kinematics, (ii) volume and traction forces, and (iii) the stress tensor into the virtual power definitions yields stress resultants (normal force, bending and torsional moments, warping-induced torsional, as well as second-, third-, and fourth-order warping-related moments) from the virtual power performed by internal forces, and beam-specific external forces (distributed forces or acting onto the cross-sectional ends of the beam, including shear forces) from the virtual power performed by external forces. Evaluating the PVP accordingly yields a set of novel equilibrium conditions, with all quantities being functions of coordinate x,

$$\begin{gathered}
-n = \frac{\mathrm{d}N}{\mathrm{d}x},\quad s_y = \frac{\mathrm{d}^2M_z}{\mathrm{d}x^2} + \frac{\mathrm{d}m_z}{\mathrm{d}x},\quad -s_z + k\left[\alpha u_z^{\text{GC}} + \beta\phi_x\right] = \frac{\mathrm{d}^2M_y}{\mathrm{d}x^2} + \frac{\mathrm{d}m_y}{\mathrm{d}x}\\
-m_{\text{T}} + k\left[\beta u_z^{\text{GC}} + \gamma\phi_x\right] = \frac{\mathrm{d}M_{\text{T}}}{\mathrm{d}x} + \frac{\mathrm{d}M_{\text{T}}^{\psi}}{\mathrm{d}x} + \frac{\mathrm{d}^2M_{\psi}^{\text{II}}}{\mathrm{d}x^2} + \frac{\mathrm{d}^3M_{\psi}^{\text{III}}}{\mathrm{d}x^3} - \frac{\mathrm{d}^4M_{\psi}^{\text{IV}}}{\mathrm{d}x^4} + \frac{\mathrm{d}m_{\psi}^{\text{II}}}{\mathrm{d}x} - \frac{\mathrm{d}^3m_{\psi}^{\text{IV}}}{\mathrm{d}x^3}
\end{gathered}$$

with α, β, and γ being elastic support-related cross-sectional properties, and the corresponding natural boundary conditions,

$$\begin{gathered}
-S_y = \frac{\mathrm{d}M_z}{\mathrm{d}x} + m_z,\quad S_z = \frac{\mathrm{d}M_y}{\mathrm{d}x} + m_y\\
m_{\psi}^{\text{II}} = -M_{\text{T}}^{\psi} - \frac{\mathrm{d}M_{\psi}^{\text{II}}}{\mathrm{d}x} - \frac{\mathrm{d}^2M_{\psi}^{\text{III}}}{\mathrm{d}x^2} + \frac{\mathrm{d}^3M_{\psi}^{\text{IV}}}{\mathrm{d}x^3} + \frac{\mathrm{d}^2m_{\psi}^{\text{IV}}}{\mathrm{d}x^2},\quad M_{\psi}^{\text{III}} = \frac{\mathrm{d}M_{\psi}^{\text{IV}}}{\mathrm{d}x} + m_{\psi}^{\text{IV}}
\end{gathered}$$

where all force quantities depend on x_i, $x_i = 0, 1$. Considering linear elasticity, and introducing the relevant rigidities allows for reformulating the PVP into a numerically evaluable format.

Cross-sectional stress distributions:

Two cross-sectional boundary problems (BVPs) give access to the shear center and the primary and secondary warping function, respectively. Together with the displacements obtained from numerical evaluation of the PVP-derived mathematical framework, the normal and shear stress distributions can be calculated [5,6].

Numerical Implementation and Concluding Remarks

Solution strategy:

In longitudinal direction of the beam, the PVP is discretized considering 1D finite elements, using both linear and cubic shape functions.

For the cross-sectional shear stress distributions, vanishing shear stress along the contour of the cross sections are considered. Their weak forms of the BVPs allow for employing standard Finite Element solution strategies, see Figure 3 for an exemplary mesh, consisting of 2308 isoparametric, quadrilateral elements [5,6], using bilinear shape functions.

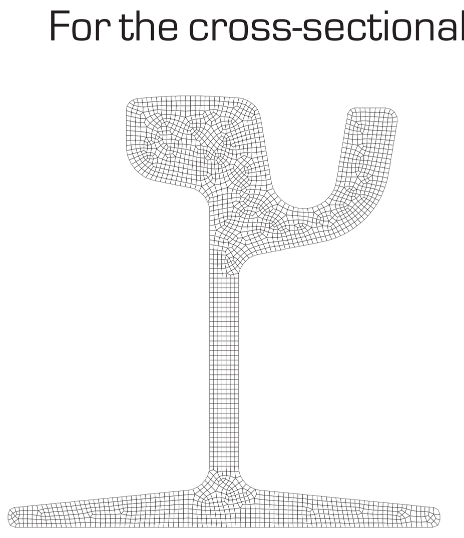

Figure 3: Exemplary Finite Element mesh, representing profile Ri60R1.

Numerical example and summary of key features:

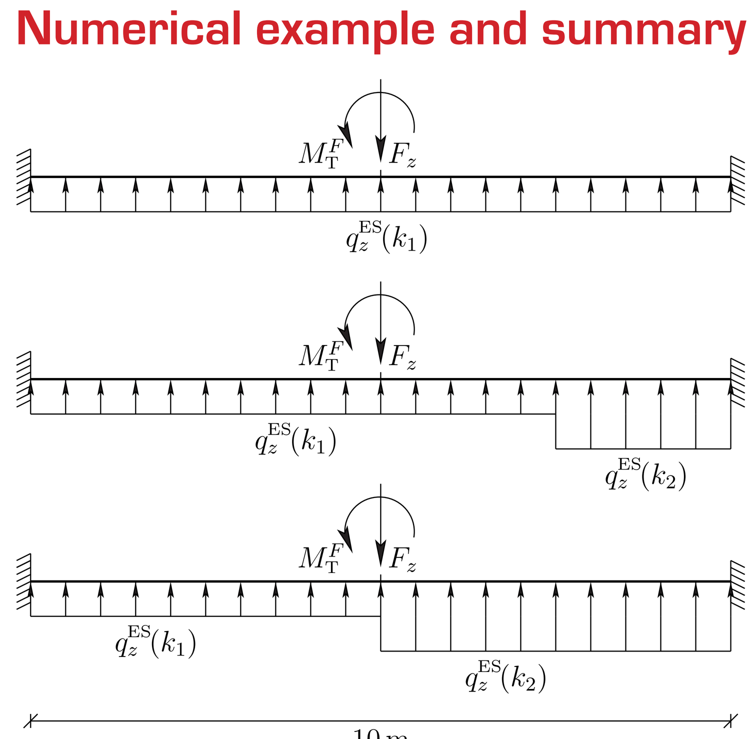

Figure 4: Tramway rails of profile Ri60R1 were studied in the form of double-clamped beams, considering different elastic support configurations.

The beam was subjected to a vertical force of $F_z \approx 60$ kN, and a load eccentricity-related torsional moment of $M_{\text{T}}^F \approx 960$ kNmm. The foundation moduli were set to $k_1 = 0.04$ and $k_2 = 1\,\text{N/mm}^3$.

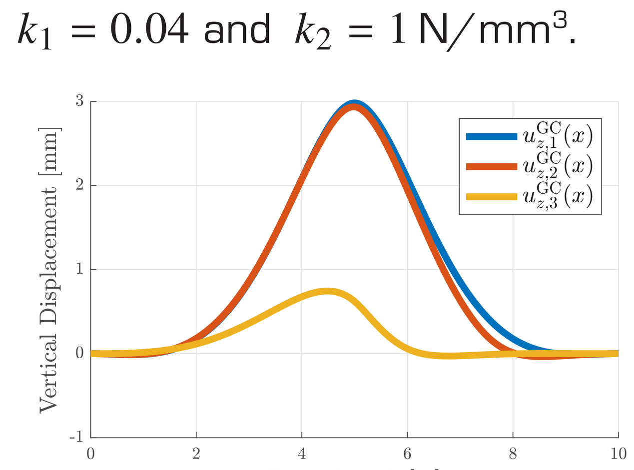

Figure 5: Computed deflections of the beam.

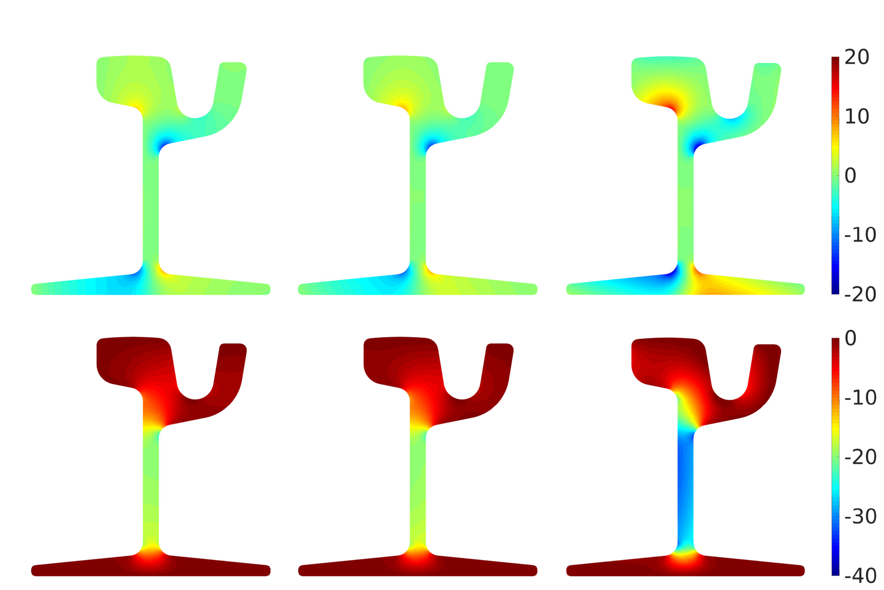

Figure 6: Computed shear stress distributions in the middle of the beam; σ_{xy} (top) and σ_{xz} (bottom); cases 1 to 3 (left, middle, right); in MPa.

- ⇨ Efficient new beam theory approach
- ⇨ Successful computational validation
- ⇨ Novel way of considering elastic support
- ⇨ Discontinuities in elastic support turn out as potential sources for rail failure
- ⇨ Model extension: temperature, eigenstresses

References and Acknowledgments

[1] Sapountzakis, ISRN Civil Eng, 2013, Art. 916581.
[2] Germain, SIAM J Appl Math, 25: 556-575, 1973.
[3] Touratier, Int J Eng Sci, 29: 901-916, 1991.
[4] Timoshenko & Goodier, Theory of Elasticity. McGraw-Hill, 1951
[5] Hasslinger et al., Engineering Structures, in production, 2019.
[6] L.C. Kourtis et al., J Mech Mater Struct, 4: 659-674, 2009.

Financial support granted by the Wiener Linien GmbH & Co KG, in the framework of the project „Investigation of the failure mechanisms relevant for grooved rails used in the Viennese tramway network", is gratefully acknowledged..